Polymer Degradation and Stability 242 (2025) 111632

Contents lists available at ScienceDirect

Polymer Degradation and Stability

journal homepage: www.journals.elsevier.com/polymer-degradation-and-stability

New insights into solid state phosphorylation of cellulose for the development of bio-based flame retardant

Sophie Dropsit, Jevgenij Lazko, Nicolas Landercy, Philippe Dubois, Fouad Laoutid *

Materia Nova Research Center, UMONS Innovation Center, Avenue Nicolas Copernic 3 B-7000 Mons, Belgium

ARTICLE INFO

Keywords:
Mechanochemistry
Cellulose
Phosphorylation
Flame retardancy

ABSTRACT

The phosphorylation of microcrystalline cellulose (MCC) has been investigated as a strategy to develop bio-based flame retardants, aiming to enhance their charring ability and thermal stability. The modification process was performed using solid-state mechanochemistry, employing varying excesses of phosphorus pentoxide (P_2O_5) to optimize the phosphorus grafting rate. It was discovered that, with a significant P_2O_5 excess, contact of the recovered blend with a small amount of water induces a vigorous reaction. This reaction leads to cellulose expansion and its conversion into a graphitic structure, while also allowing for the grafting of a high phosphorus content. This phosphorylated graphitic cellulose demonstrated a superior flame retardant effect in polypropylene (PP), achieving a 55 % reduction in peak heat release rate (pHRR) even at a relatively low incorporation content (12.5 wt.%), while also conserving composite ductility.

1. Introduction

The development of bio-based flame retardants has attracted significant interest in recent decades. This approach seeks to leverage agroresources for high value technical applications while also for supporting the development of low-carbon footprint materials. Various natural products, derived from plants or animals, have been studied and have shown effective flame-retardant properties in multiple materials [1–4].

These bio-based flame retardants are typically developed through the chemical modification of bioadditives with an inherent ability to form charred structures during their thermal degradation. They can also be valuable when combined with other flame retardants, such as metallic hydroxides[5,6], phosphorus and nitrogen-based compounds [7–9].

The phosphorylation of bioadditives, such as lignin[10,11], cellulose [12–14], and tannins[15,16], is the most widely used method to enhance their flame-retardant effect. The presence of phosphorus-containing groups improves both the char yield and its thermal stability through condensation reactions involving the hydroxyl groups of the phosphorus functions and those of the bioadditives.

The formation of this char is a key mechanism in the action of these additives, which primarily act in the condensed phase. The formation of a stable char layer on the surface of the burning material acts as a protective barrier, shielding the underlying layers from direct flame exposure and reducing heat transfer. Additionally, it limits the production of combustible volatiles and their migration to the combustion zone, further enhancing fire protection.

Cellulose is the most abundant bio-based material and is available at a very affordable cost. It exists in various forms, both nano and micro, but microcrystalline cellulose (MCC) is the easiest to incorporate into thermoplastic polymers, as it comes in a powder form that is easy to handle for melt compounding.

The phosphorylation process must be sustainable to preserve the environmental benefits of biobased flame retardants (FRs). This could be achieved using eco-friendly phosphorus-based reagents such as phytic acid [17] or by avoiding using methods that consume excessive energy, rely on organic solvents, or involve corrosive or toxic chemicals. This is crucial as these practices undermine sustainability. Thus, there is a pressing need to innovate and adopt environmentally friendly alternatives to traditional phosphorylation processes.

Recently, mechanochemistry has emerged as an eco-friendly process that enables efficient chemical reactions without the use of solvents[18]. A mechanochemical reaction is a chemical reaction induced by the direct absorption of mechanical energy, which can result from impact, tension, or friction. The input of mechanical energy into chemical reactions is highly significant and can lead to new products distinct from those obtained through conventional solvent-based chemical reactions.

* Corresponding author.
E-mail address: fouad.laoutid@materianova.be (F. Laoutid).

https://doi.org/10.1016/j.polymdegradstab.2025.111632
Received 25 June 2025; Received in revised form 27 August 2025; Accepted 28 August 2025
Available online 28 August 2025

This mechanical energy enhances the probability of collisions between reactants, promoting a homogeneous reaction environment, preventing concentration gradients of products, and dissipating localized heat. Mechanical impacts also break down large particles, thereby creating more surface area and generating structural defects and new reactive sites[19]. Ball milling is a highly effective mechanochemical technique due to its affordability, ease of implementation, and ability to handle large quantities. The high-speed rotation of the milling balls creates shear forces and raises the temperature of the reaction mixture[20]. Temperature control in a simple ball mill is not feasible, but new equipment and technologies are being developed to support the growth of this sector. For example, the Mechanochemical Reactor WAB IMPACT REACTOR from the WAB GROUP® can regulate temperature (both heating and cooling) and is designed for continuous operation.

We recently reported two examples of the use of mechanochemistry, particularly ball milling, to chemically modify two biobased additives, i.e. tannic acid[21] and (micro)cellulose[22] with phosphorus pentoxide (P_2O_5). In both cases, the phosphorylation reaction was successful within a short time frame (60 min) and led to the development of effective flame retardants in polypropylene. In the case of tannic acid, chemical modification by ball milling achieved a phosphorus grafting rate similar to that obtained using conventional organic chemistry method in solvent phase (around 2 wt.%). However, for MCC, the results were not comparable, as a low grafting rate (4.15 wt.%) was obtained by ball milling, in contrast to the 16.5 wt.% P content achieved through modification in solvent phase. It is important to note that even the starting reagents differ in each case, this comparison mainly underscores that, in the case of cellulose, ball milling modifies only a small fraction of its hydroxyl groups, yielding a degree of substitution (DS) of 0.25, which is significantly lower than the DS of 1.3 achieved when cellulose is phosphorylated using phosphonic acid and urea as catalysts at 150 °C for 2 h[23]. This difference appears to be related to the size and structure of cellulose, that present compact macromolecular structure, with only the particle surface being accessible for modification, whereas tannic acid, being a smaller molecule, is more readily available to react with P_2O_5.

In this study, we aim to gain deeper insight into the key parameters governing the ball-milling phosphorylation of cellulose using P_2O_5. In particular, we investigate how varying the P_2O_5 content influences the phosphorus grafting efficiency, structural modifications of cellulose, and its thermal properties. Furthermore, we assess the impact of these modifications on both the flame-retardant performance and the mechanical properties of polypropylene composites incorporating the phosphorylated cellulose.

2. Materials and methods

2.1. Materials

The polypropylene (PP) utilized in this study is a high-impact-modified copolymer (PP PHC26) designed for injection molding applications, from SABIC Europe B.V. (Sittard, The Netherlands) and supplied by RESINEX (Arendonk, Belgium). Microcrystalline cellulose and phosphorus pentoxide (P_2O_5, 99 % purity) were purchased from Sigma Aldrich (Burlington, MA, USA).

2.2. Preparation of phosphorylated cellulose

Cellulose was chemically modified with P_2O_5 via ball milling using a PM 400 planetary mill (Retsch, Haan, Germany), following the procedure described by Maadouz et al [24]. Microcrystalline cellulose (MCC) and P_2O_5 were physically mixed and placed in a 500 mL stainless steel jar, together with 60 stainless steel balls. The mixture was processed at room temperature at a rotation speed of 200 rpm. Three different MCC/P_2O_5 weight ratios (90/10, 70/30, and 43/57) were employed, corresponding to P_2O_5 contents equivalent respectively to 0.25; 1 and 3 times the hydroxyl groups content of MCC. The resulting modified celluloses were designated as MCC-P1, MCC-P2, and MCC-P3, respectively. Milling was carried out for 1 hour, with a 30 secondes pause every 10 minutes.

2.3. Preparation of PP composites

PP and additives were previously dried at 60 °C for 24 hours, prior to be melt processed in a Brabender Plastograph (W50EHT-3, Germany) for 10 minutes (3 minutes mixing at 30 rpm and 7 minutes at 90 rpm) at 180 °C. The blends were compression molded into plates measuring 10 × 10 × 0.3 cm^3. Some of these plates were used for Mass Loss Cone (MLC) tests, while others served as the source for specimens used in mechanical testing, which were cut using hydraulic bench press HESS 5MP (Richard Hess MBV Gmbh, Germany). This compression molding process was carried out using an Agila PE20 hydraulic press, at 200 °C, according to the following procedure: Initially, the sample is placed on the heated section of the press for 3 minutes and subjected to a pressure of 10 bar for 3 minutes and 20 secondes. This is followed by three degassing steps. The sample is then pressed again at 150 bar for 2 minutes and 30 secondes, and finally transferred to the cold section of the press, where it is maintained under pressure for 5 minutes. Table 1 presents the identification codes and corresponding chemical compositions of the investigated samples.

2.4. Methods of characterization

The thermal stability of pristine MCC and its derivatives as well as PP, and their corresponding composites was evaluated through thermogravimetric analysis (TGA) using a TGA II instrument (Mettler Toledo, Greifensee, Switzerland). For each test, approximately 5 mg of material was heated from 30 °C to 800 °C at a constant rate of 10 °C·min^{-1}. Modified MCC samples were analyzed under both nitrogen and air atmospheres, whereas composite samples were tested only in air.

FTIR spectra were obtained using a Bruker ALPHA II spectrometer (Bruker Optics, Ettlingen, Germany), operating in the 4000–400 cm^{-1} wavenumber range, with a resolution of 2 cm^{-1} and averaging over 32 scans. Raman spectra were recorded using a micro-Raman system (Senterra Bruker Optik GmbH, Massachusetts, USA) with a laser wavelength of 532 nm and a power of 10 mW.

Phosphorus content in the modified cellulose was determined using inductively coupled plasma (ICP) analysis, carried out with an Optima 7300dV ICP-OES instrument from Perkin Elmer (Waltham, MA, USA). Prior to analysis, the sample was digested with nitric acid. Phosphorus concentrations were quantified using calibration curves derived from ICP measurements of standard solutions at concentrations of 5 and 10 ppm, alongside unmodified cellulose as a reference.

The phosphorus content determined by ICP allows the calculation of the average number of grafted groups per monomer unit of cellulose, known as the degree of substitution (DS), which can be estimated using an empirical formula reported in the literature[25].

$$DS = \frac{Mcellulose \times P\%}{100 \times M(P) - \Delta M \times P\%}$$

$M_{cellulose}$ is the molar mass of the cellulose d-glucose unit (162 g/

Table 1
Content (Expressed in wt%) of PP and Additives used to prepare the different compositions.

Sample label	PP	MCC	MCC-P1	MCC-P2	MCC-P3
PP	100	—	—	—	—
PP-30MCC	70	30	—	—	—
PP-12.5MCC	87.5	12.5	—	—	—
PP-30MCC-P1	70	—	30	—	—
PP-30MCC-P2	70	—	—	30	—
PP-12.5MCC-P3	87.5	—	—	—	12.5

mol), P % is the phosphorus weight percentage in the modified cellulose (e.g., 4.15 wt.%), M(P) is the molar mass of phosphorus (31 g/mol), and ΔM is the mass difference between the grafted group and the leaving group (97 g/mol, corresponding to $M(H_3PO_4) - M(H)$).

Scanning electron microscopy coupled with energy dispersive X-ray analysis (SEM-EDX) was employed to assess the morphology of phosphorylated celluloses as well as their dispersion within PP matrix. The analysis was conducted using a Hitachi SU-8020 instrument (Hitachi, Tokyo, Japan). The presence of internal porosity into modified cellulose particles was also investigated by SEM. The sample was embedded in an epoxy resin, polished using Leica TIC3X ion polisher (from Leica Microsystems, Wetzlar, Germany) at an accelerating voltage of 7 kV prior analysis.

Tensile tests were performed according to ISO 527 standard on a Llyod LR 10 K equipment. The tests were conducted on type V samples of ASTM D638 standard, at a temperature of 23 °C, relative humidity of 50 % and with a cross-head speed of 10 mm/min and a 1000 N force cell. Five specimens of each sample were tested to determine the mean value of the results.

The fire behavior of PP and its composites was assessed using a mass loss cone (MLC) apparatus from Fire Testing Technology (East Grinstead, West Sussex, UK), in accordance with the ISO 13927 standard. Samples (100 × 100 × 3 mm^3) were subjected to an external heat flux of 35 $kW.m^{-2}$ corresponding to common heat flux in a mild fire scenario. Heat Release Rate (HRR) was measured as function of time, and Time To Ignition (TTI), Total Heat Release (THR) and peak of Heat Release Rate (pHRR) were determined.

3. Results and discussion

3.1. Solid state phosphorylation of cellulose

3.1.1. Structural characterization

Different grades of phosphorylated cellulose were obtained using the same ball milling procedure, but with varying MCC / P_2O_5 ratios. The first observation is that the phosphorylated celluloses MCC-P1 and MCC-P2 retain their white color, whereas the batch with a large excess of P_2O_5 (MCC-P3) undergoes a very radical transformation, becoming black and expanded as evidenced on Fig. 1. It can be observed that the MCC-P3 mixture already appears darker after just 10 min of exposure to air, whereas the MCC-P1 and MCC-P2 mixtures remain white, even after washing with water. The radical colour change occurs rapidly upon exposure of MCC-P3 to a small amount of water (some drops). In fact, upon contact with water, the MCC-P3 sample undergoes an instantaneous blackening reaction, which is highly exothermic and accompanied by significant expansion and the release of acidic vapors. For safety reasons, this step was conducted under a properly ventilated fume hood.

FTIR spectra (Fig. 2) of both MCC-P1 and MCC-P2 show no significant differences compared to that of untreated cellulose. Similar observations have previously been reported for cellulose modified via mechanochemical treatment with P_2O_5, where the absence of spectral changes was attributed to a low degree of phosphorus grafting [24].

Chemical modifications in the MCC-P3 sample, typical for thermal cellulose degradation, can be observed by FTIR as well. Characteristic cellulose C—O deformation band of primary alcohol at 1030 cm^{-1} is not predominant anymore. C—O and C—O-C peaks at 1260 and 1160 cm^{-1} are not well observable, neither. Thermal degradation due to the mechanochemical treatment with P_2O_5 also induced a decrease in 1640 cm^{-1} peak corresponding to OH bending. Thus, the new predominant peak at this region is that at 1584 cm^{-1} corresponding most probably to the formation of conjugated $C = C$ bonds. High intensity peaks are also visible in 870–750 cm^{-1} region typical for the aromatic $C = C$ [26–28].

To gain further insight into the structure of MCC-P3, Raman spectroscopy analyses were performed. In fact, the structural organization of carbon-based materials could be assessed by this technique, particularly through the identification of two main bands: one near 1389 cm^{-1} (D band - D standing for disorder), associated with disordered or amorphous carbon, and another near 1598 cm^{-1} (G band - G standing for graphite), related to graphitized structures [29,30]. The D band is attributed to the vibration of carbon atoms with dangling bonds at the planar ends of disordered graphite or glassy carbon while the G band is originated by the vibration of sp^2-hybridized carbon atoms in the

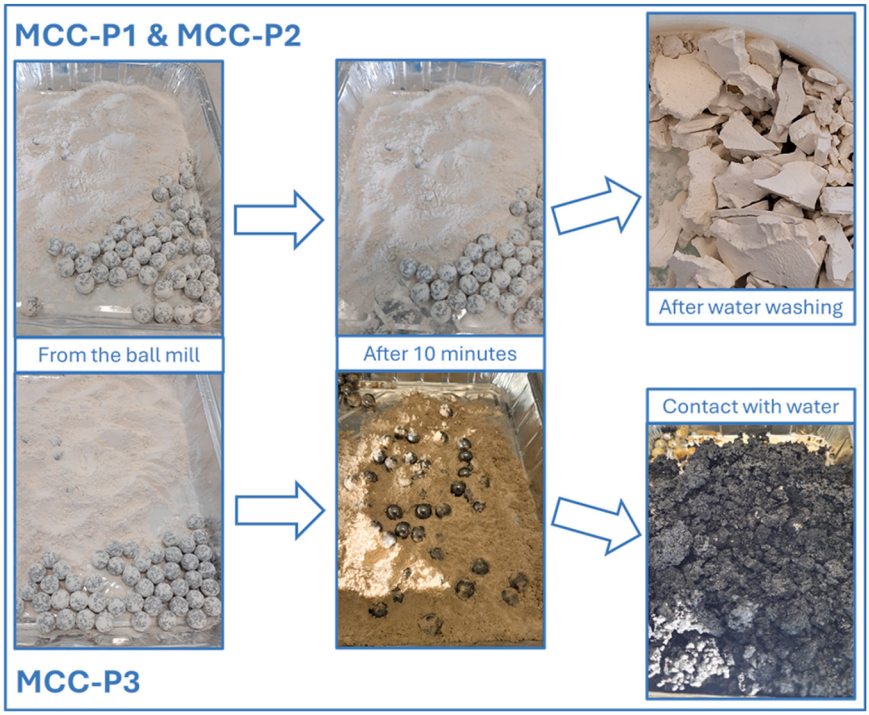

Fig. 1. Images showing the effect of the cellulose/P_2O_5 ratio on the general appearance of the modified cellulose at the exit of the ball mill, after 10 min and after washing or brief contact with water.

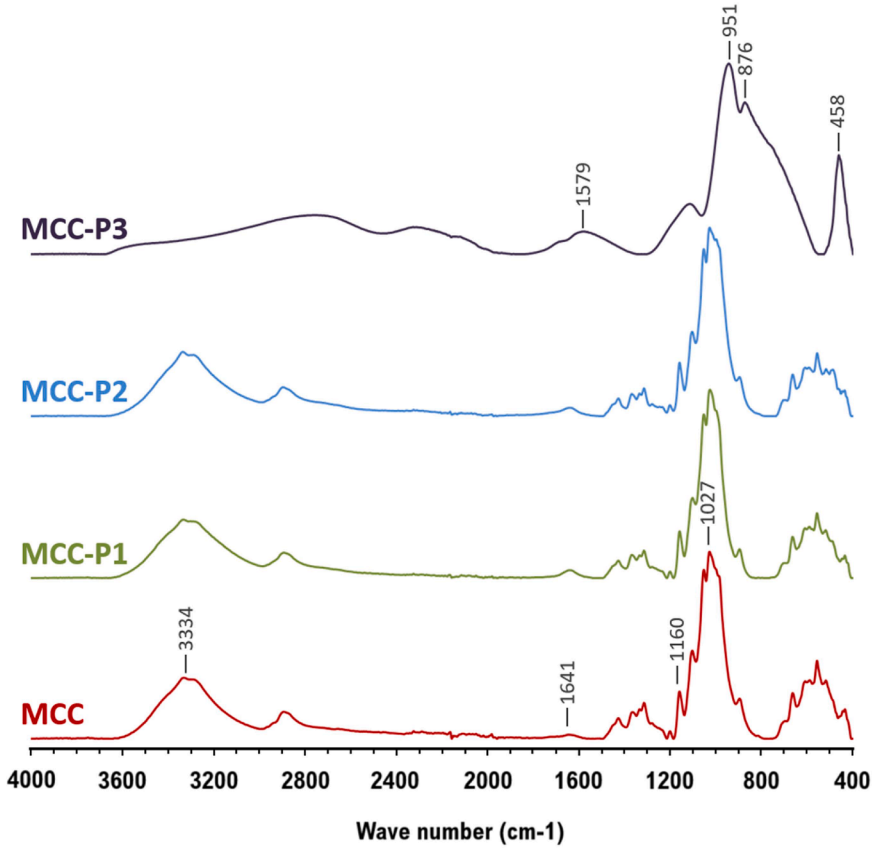

Fig. 2. FTIR spectra of pristine MCC and its derivatives.

graphite layer and to the E_{2g} mode of hexagonal graphite [31,32]

Fig. 3 presents the Raman spectrum of MCC-P3 cellulose confirming the presence of both the D and G bands. Moreover, the intensity ratio of these bands (I_D/I_G) provides insights into the structural quality of the carbon material. For MCC-P3, the I_D/I_G ratio is 0.74, indicating a graphitic structure with a moderate level of defects. Raman spectroscopy analysis clearly indicates that the black coloration of MCC-P3 cellulose results from the transformation of cellulose into graphitic carbon structures.

At the macroscopic level, SEM observations provide insights into the evolution of particle size subsequent to the treatment (Fig. 4). The images of cellulose particles confirm the effect of excess P_2O_5, which

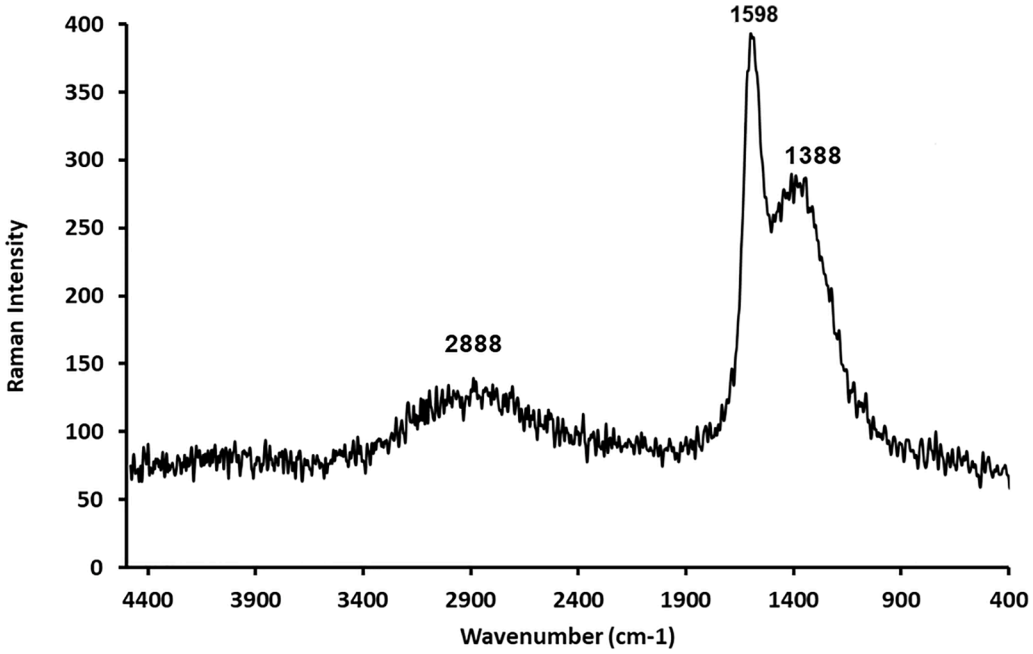

Fig. 3. Raman spectrum of MCC-P3.

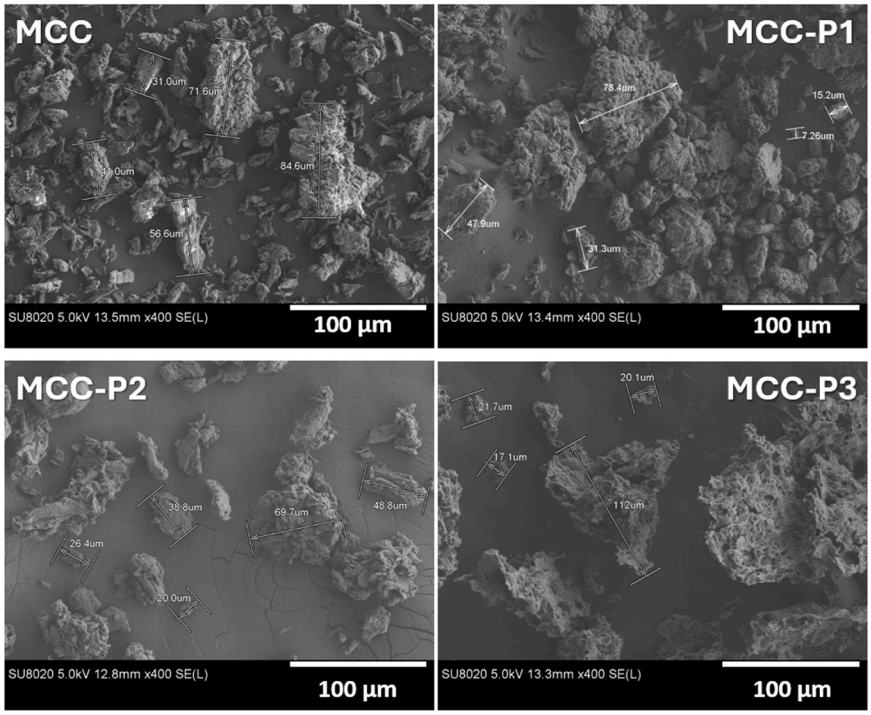

Fig. 4. Images showing the effect of the cellulose/P_2O_5 ratio on the general appearance of the cellulose particles.

induces larger dimensions as compared to either native cellulose or MCC-P1 and MCC-P2, due to the expansion observed in the contact of MCCP-3 with water. This expansion and its impact on internal structure were further investigated by SEM analysis of particles embedded in epoxy resin. Polishing of the cellulose/epoxy composites allowed for detailed examination of the particle internal morphology. These images clearly demonstrate that the presence of excess P_2O_5 induces the formation of internal porosity within the MCC-P3 particles (Fig. 5). The observed porosity underscores the cellulose expansion driven by the vigorous cellulose dehydration reaction induced by P_2O_5.

The use of a large excess of P_2O_5 not only induces a color change, substantial cellulose expansion, and its transformation into graphitic structure, but also results in a significantly higher phosphorus grafting rate. ICP analysis (Table 2) reveals that MCC-P3 contains 17.3 wt.% phosphorus, corresponding to a degree of substitution (DS) of approximately 1.97 %. In comparison, significantly lower phosphorus contents are observed for MCC-P1 and MCC-P2, at 1.1 % and 3.6 %, respectively, corresponding to DS values of 0.06 % and 0.21 %. The grafting rate achieved for MCC-P3 is particularly remarkable, ranking among the highest reported values for cellulose phosphorylation in the literature, with previously reported values including 0.63 wt.%[33], 1.92 wt.% [34], 4.40 wt.%[24], 13.22 wt.%[35], 16.50 wt.%[23] and 20 wt.% [36].

Table 2
TGA Parameters, P content and DS for cellulose and derivatives.

	Residue at 400 °C (%)		Residue at 500 °C (%)		P (wt. %)	DS (%)
	Air	N_2	Air	N_2		
MCC	19	13	6	10	0	0
MCC-P1	34	41	15	35	1.1	0.06
MCC-P2	44	47	30	43	3.6	0.21
MCC-P3	75	71	67	66	17.3	1.97

The conversion of cellulose into charring structures has previously been reported under the action of acids such as phosphoric acid [37] or sulfuric acid [38], but only above 200 °C. To the best of our knowledge,

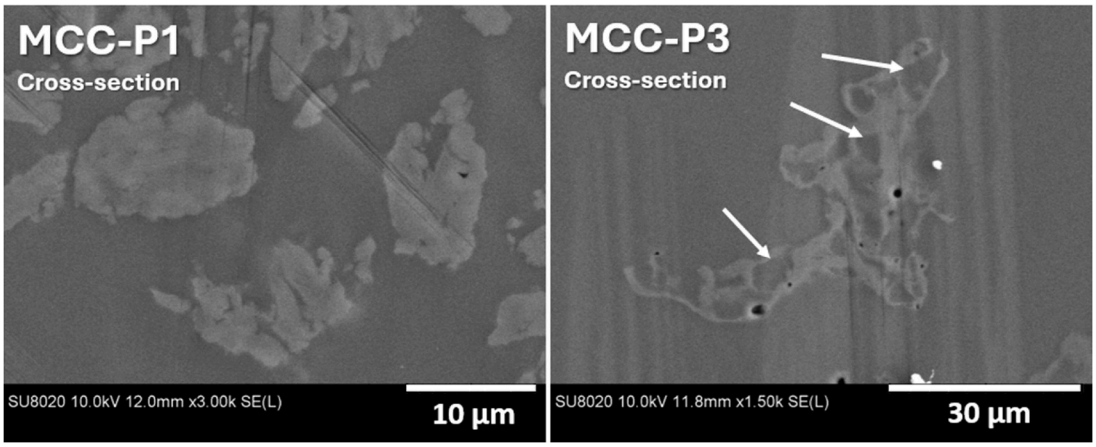

Fig. 5. SEM images of polished cross-sections of MCC-P1 and MCC-P3 particles embedded in epoxy resin.

no study has reported the formation of graphitic structures from cellulose at room temperature. The reactions leading to cellulose carbonization are well-known and involve cellulose dehydration processes, resulting in the formation of dehydrated cyclic structures in the solid phase during pyrolysis[39,40].

In our case, both carbonization and graphitization of cellulose start at room temperature upon the addition of a small amount of water to a specific cellulose/P_2O_5 mixture, namely, the one yielding MCC-P3. This MCC-P3 grade thus demonstrates strong potential as a condensed-phase flame retardant in thermoplastic polymers.

This reaction was only made possible through mechanochemistry, which eliminates the need for solvents. Solvent-based approaches would not allow for the rapid dehydration of cellulose by P_2O_5 in the presence of a small amount of water. Indeed, in solvent-based reactions, a filtration step is typically required to remove excess reagent, which would have prevented the charring reaction observed in our system.

The thermal stability of the char as well as its resistance to thermal and thermo-oxidative degradation are key factors influencing the flame-retardant efficiency of a condensed-phase mechanism. These parameters were evaluated in the next section by TGA for MCC-P3 cellulose and compared to those of the other cellulose grades.

3.1.2. *Thermal stability*

The effect of cellulose phosphorylation on its thermal stability was assessed using thermogravimetric analyses under both air and nitrogen atmospheres. Weight loss curves versus temperature are depicted in Fig. 6, with corresponding data summarized in Table 3.

Unmodified cellulose degrades differently depending on the atmosphere used. Under air, its decomposition occurs in two stages. The first stage, around 320 °C, leads to char formation, which is susceptible to thermo-oxidative degradation, hence the presence of a second degradation step in air, but not under nitrogen. It is also worth noting the occurrence of a weight loss around 50 °C, observed across all types of cellulose, which may be attributed to the presence of physiosorbed water.

Table 3
TGA data for the different cellulose grades as determined from thermograms recorded under air and nitrogen atmospheres and using a heating rate of 10 °C·min^{-1}.

	Main decomposition temperatures (°C)		Residue at 400 °C		Residue at 500 °C	
	air	**N_2**	**air**	**N_2**	**air**	**N_2**
MCC	320; 500	340	20	13	5.5	10
MCC-P1	256; 495	270	36	40	16	35
MCC-P2	235; 585	240	44	47	29	42
MCC-P3	170; 580	180; 580	73	71	66	66

In the case of phosphorylated cellulose samples, the shape of the weight loss curves differs not only from that of native cellulose, but also between the phosphorylated samples themselves, under both air and nitrogen atmospheres. This behavior is strongly influenced by the phosphorus grafting level. For phosphorylated celluloses MCC-P1 and MCC-P2, the first degradation step occurs earlier and at significantly lower temperatures compared to native cellulose. Under air, the onset of this first degradation step is observed at 256 °C for MCC-P1 and 235 °C for MCC-P2, compared to 320 °C for unmodified cellulose. Under nitrogen, MCC-P1 and MCC-P2 decompose at 270 °C and 240 °C, respectively, while native MCC decomposes at 340 °C.

The premature thermal degradation observed in phosphorylated celluloses is attributed to the presence of phosphoric acid groups, which trigger early decomposition of the cellulose, a phenomenon widely reported in the literature [41]. Phosphoric acid promotes dehydration of the cellulose, along with internal rearrangement reactions, leading to the formation of dehydrated cyclic char structures.

The primary decomposition step of phosphorylated cellulose leads to the formation of a more thermally stable char compared to that produced during the degradation of unmodified cellulose. This is reflected in the TGA curves by a significantly higher amount of residual mass.

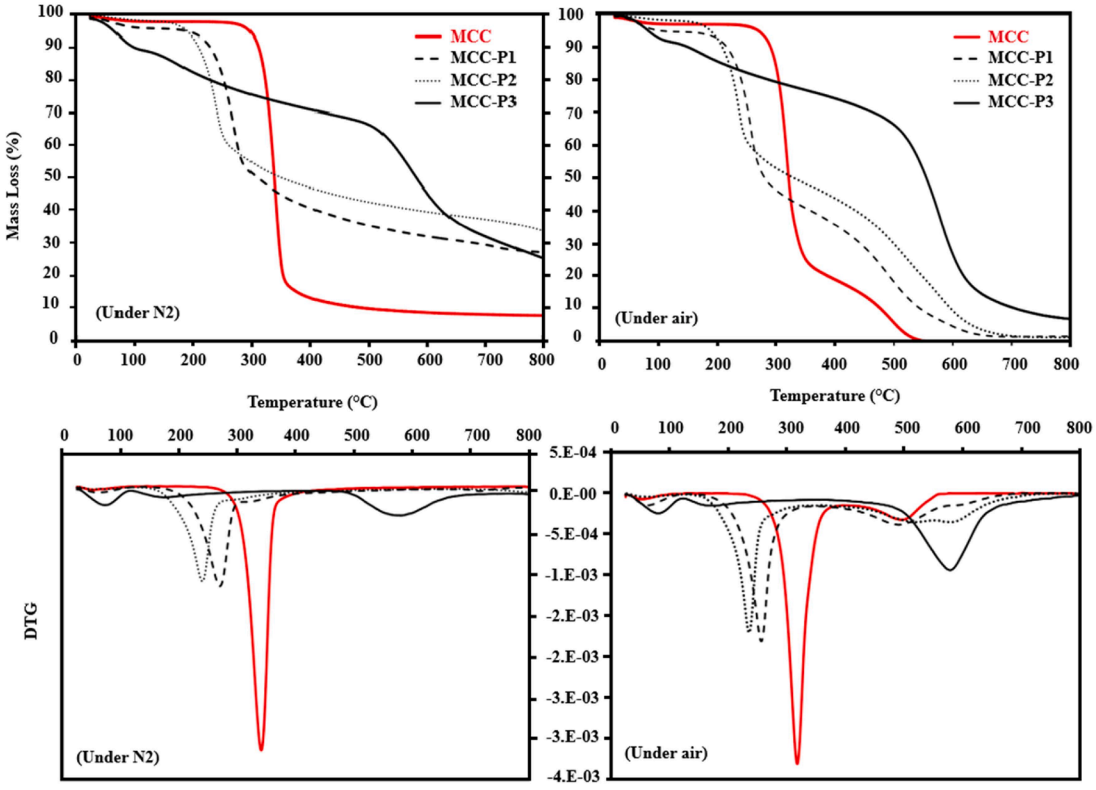

Fig. 6. TGA and DTG curves of untreated and phosphorylated celluloses, under N_2 and air, at 10 °C.min^{-1}.

Under air, the residue at 400 °C increases in the presence of phosphorus, rising from approximately 20 % for native MCC to around 36 % and 44 % for MCC-P1 and MCC-P2, respectively. Under N_2, the same trend is observed, with similar residue yields, i.e., 40 % for MCC-P1 and 47 % for MCC-P2. This enhanced thermal stability of the two phosphorylated celluloses compared to native cellulose is also observed at higher temperatures.

However, the most pronounced effect is observed with MCC-P3. The shape of the mass loss curve for this cellulose is completely different from that of the other three samples. A significantly earlier degradation is observed, and MCC-P3 started to lose weight from 50 °C with around 10 % of weight loss at 100 °C. Given the significant mass loss observed, this loss cannot be attributed solely to water adsorbed in the porous structure of cellulose, especially since the sample was dried prior to analysis. Instead, it suggests that a portion of degraded cellulose is being carried away by the analysis gas flow (air or N_2), likely due to its low density. Moreover, thermal degradation of MCC-P3 leads to a much higher residue yield, around 70 % at 400 °C and 66 % at 500 °C. The amount of residue formed, whether under air or nitrogen, is much higher with MCC-P3 than those obtained with the two phosphorylated celluloses, MCC-P1 and MCC-P2. The MCC-P3 cellulose grade, which contains a high level of grafted phosphorus, exhibits a strong ability to form thermally stable char.

3.2. PP / cellulose composites properties

The different cellulose grades were incorporated into PP at a loading rate of 30 wt.% via melt processing, with the exception of MCC-P3. Its low bulk density, caused by expansion following the contact with traces of water after ball milling, prevented successful incorporation at that high concentration. For this grade, it was only possible to prepare a blend with a maximum of 12.5 wt.% loading.

3.2.1. Particle dispersion

The functional performance of composites is highly dependent on the distribution of the minor phase. For all PP-based compositions incorporating native and phosphorylated cellulose particles, processed using a Brabender internal mixer, it was crucial to assess how well the particles were dispersed within the matrix. SEM was therefore employed to evaluate the filler dispersion, as insufficient dispersion could diminish the flame-retardant effectiveness of the additive and compromise the overall properties of the composite. SEM micrographs obtained in chemical contrast mode are presented in Fig. 7. These images indicate that ball milling induces a reduction in cellulose particle size and homogeneous dispersion throughout the polymer matrix. It is important to note that the PP + 12.5 wt.% MCC-P3 blend contains a lower cellulose content, which accounts for the reduced presence of particles observed in the corresponding SEM micrograph.

3.2.3. Composite thermal stability

The thermal stability of the composites was evaluated using TGA under air (Fig. 8 and Table 4). The curves clearly indicate that the thermal behavior of the composites depends on the type of cellulose incorporated. In general, the presence of cellulose particles, regardless of their type, promotes an earlier onset of composite degradation. This effect is attributed to the thermal decomposition of cellulose, which occurs at lower temperatures than that of the polymer matrix, and is further enhanced when the cellulose is phosphorylated (Fig. 6). Notably, the degradation of composites containing phosphorylated celluloses (MCC-P1 and MCC-P2) starts at lower temperatures (290 °C and 370 °C, respectively) than that of the composite with native cellulose (360 °C). It is important to note that the premature degradation of MCC-P3 does not lead to early degradation of the composite, likely due to its low incorporation rate and the absence of chemical interactions with the polypropylene matrix. However, among the various formulations, only the composite containing MCC-P3 exhibits higher thermal stability than neat polypropylene (PP) beyond 350 °C. This composite also retains a significant char yield of approximately 20 % at 420 °C, which decomposes gradually with increasing temperature. Above 420 °C, the two composites containing 30 wt.% MCC-P2 and 12.5 wt.% MCC-P3 exhibit very similar char degradation profiles.

3.2.4. Flame retardant properties

The flammability behavior of the materials was evaluated using Mass Loss Cone calorimetry, a widely adopted bench-scale method for assessing fire performance. Experiments were conducted under an

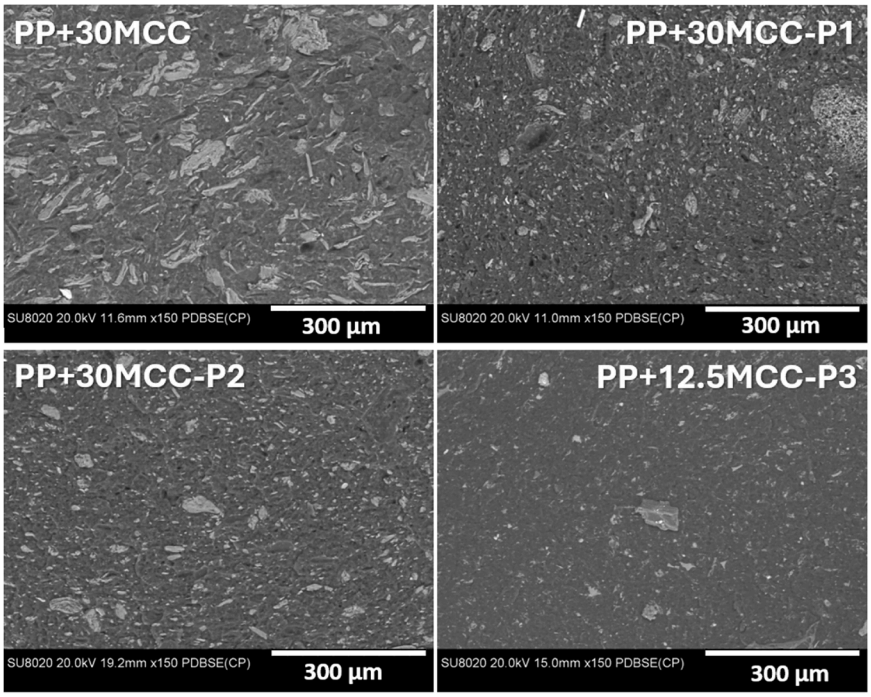

Fig. 7. SEM micrographs of cryo-fractured surface of the different PP / cellulose composites.

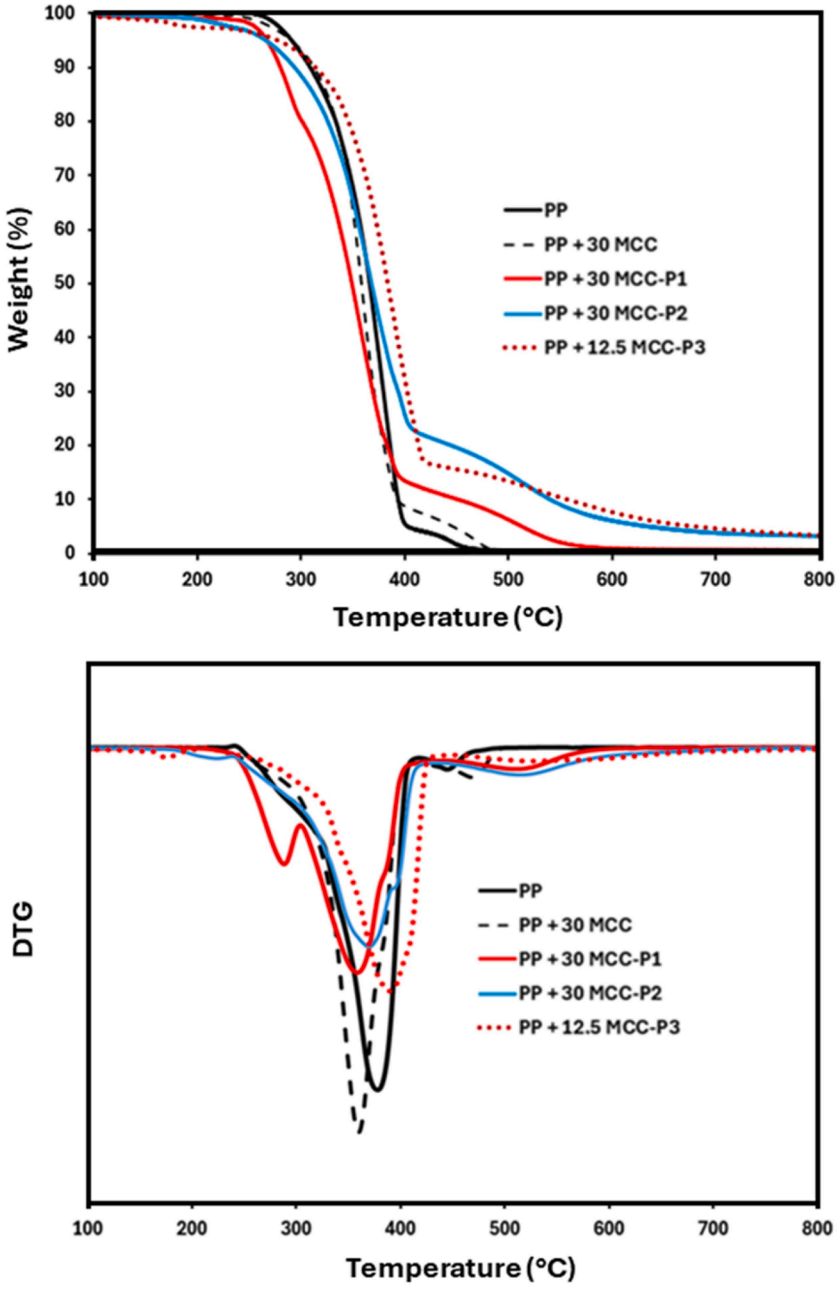

Fig. 8. TGA and DTG curves of PP and PP-Cellulose composites under air at 10 °C.min^{-1}.

Table 4
TGA date under air for PP and the different composites at a heating rate of 10 °C·min^{-1}.

Composition	Main decomposition temperatures (°C)	Residue at 500 °C (%)	Residue at 700 °C (%)
PP	380 ; 445	0	0
PP + 30-MCC	360	0	0
PP + 30-MCC-P1	290 ; 360 ; 515	6.6	0
PP + 30-MCC-P2	370 ; 400 ; 518	14.4	3.8
PP + 12.5-MCC-P3	390 ;	13.4	4.6

external heat flux of 35 kW.m^{-2}, representative of moderate fire exposure conditions. Key fire parameters, namely the peak heat release rate (pHRR), time to ignition (TTI) and total heat release (THR), were analyzed due to their critical relevance in characterizing ignition behavior and fire growth potential. High pHRR values combined with short TTI are indicative of rapid ignition and accelerated flame spread. The HRR profiles obtained from the Mass Loss Cone calorimeter tests are depicted in Fig. 9, while the corresponding quantitative data are compiled in Table 5.

Neat PP exhibited intense combustion, characterized by a sharp HRR peak reaching a pHRR of 910 kW·m^{-2} at 200 s, with complete degradation with no residual char. The addition of 30 wt.% microcrystalline cellulose (MCC) did not significantly alter the HRR curve, though a slight decrease in pHRR was observed, accompanied by a shorter ignition time (45 s), indicative of reduced ignition resistance due to the flammability of cellulose. When phosphorylated cellulose was

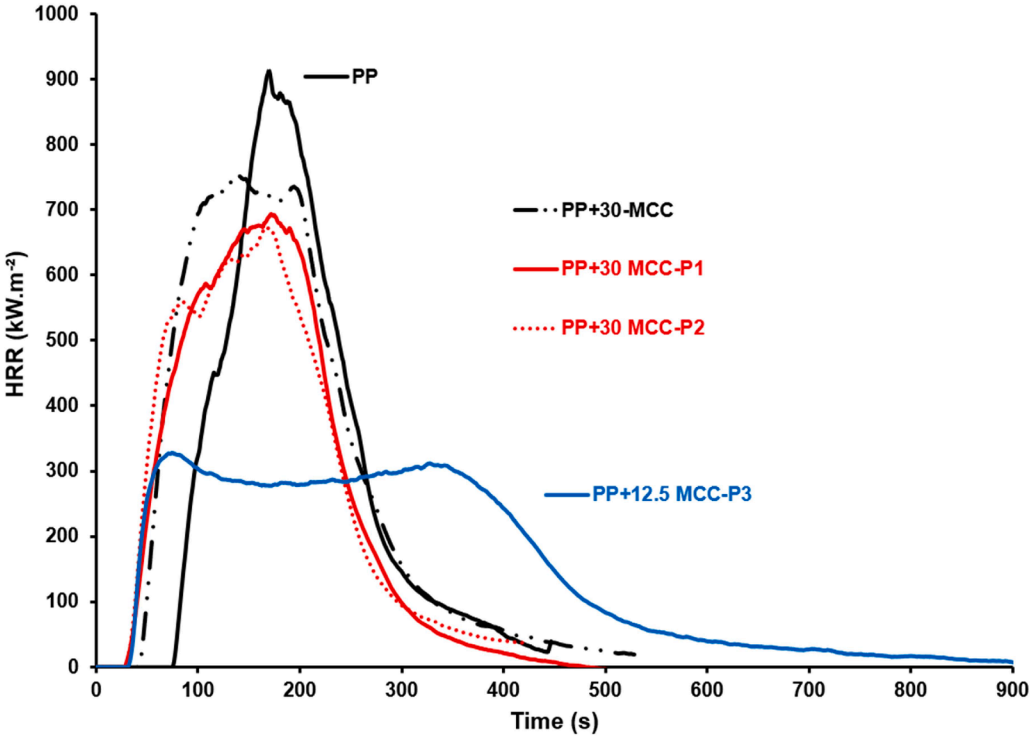

Fig. 9. HRR curves of neat PP and PP composites, obtained by mass loss cone calorimeter at 35 kW.m^{-2}.

Table 5
Mass Loss Cone calorimeter test results of neat PP and PP–cellulose-based composites.

Composition	TTI (s)	pHRR (kW.m^{-2})	pHRR variation (%)	THR (MJ.m^{-2})
PP	63 ± 4	910 ± 70	—	108 ± 20
PP + 30-MCC	45 ± 10	760 ± 15	−16	110 ± 40
PP + 30-MCC-P1	40 ± 10	710 ± 5	−22	105 ± 30
PP + 30-MCC-P2	31 ± 4	680 ± 10	−25	95 ± 25
PP + 12.5-MCC-P3	38 ± 10	410 ± 70	−55	105 ± 25

introduced (MCC-P1 and MCC-P2, containing 1.1 % and 3.6 % phosphorus, respectively), only a minor reduction in pHRR was recorded. However, the ignition time further decreased respectively to 40 and 31 s, which can be attributed to the reduced thermal stability of phosphorylated cellulose, as supported by TGA results (Fig. 6).

The most pronounced flame-retardant effect was achieved with MCC-P3, which, despite being incorporated at only 12.5 wt.%, induced a drastic alteration of the HRR profile and a remarkable reduction in pHRR of approximately 55 %. This exceptional performance is primarily attributed to the high phosphorus content of MCC-P3, resulting in a total phosphorus loading of 3.6 wt% in the composite, significantly higher than the ~1 wt% achieved with 30 wt% of MCC-P2. The efficient flame-retardant action of MCC-P3 is further reinforced by its graphitized structure, which facilitates the rapid formation of a cohesive, thermally stable char layer during combustion. This char acts as a protective barrier, reducing heat and mass transfer and thereby mitigating fire propagation.

The THR is influenced by the blend composition. The incorporation of 30 wt.% unmodified cellulose into PP do not leads to any significant change in THR, that remain around 110 MJ·m^{-2}. This behavior was also confirmed in the presence of the three phosphorus-modified cellulose grades. Their incorporation does not lead to any significant reduction in THR, mainly because the entire composites ultimately undergoes complete degradation during combustion (Figs. 10 and 11), and also due to the relatively low loading of MCC-P3, incorporated at only 12.5 wt.%. The composite containing 12.5 % MCC-P3 exhibits a total heat release comparable to that of neat PP, but spread over 500 s instead of only 200 s, along with a significantly reduced pHRR, actually decreased by 55 %.

The elevated phosphorus content is a key factor in promoting char formation and enhancing the thermal stability of the composite. However, it is the synergistic combination of high phosphorus loading and the graphitized structure of MCC-P3 that proves to be decisive. This combination enables for the formation of insulating char, that reduces the mass loss rate during combustion. This dual action, physical protection by graphitic carbon structures and chemical reinforcement by phosphorus species, forms the basis of the outstanding flame-retardant performance observed in MCC-P3-based composites.

3.2.5. *Mechanical properties*

One of the major challenges in the flame retardant treatment of polymeric materials is to achieve an optimal balance between fire performance and the preservation of other functional properties. Among these, mechanical properties, particularly ultimate tensile strength and elongation at break, are often significantly compromised upon the incorporation of flame retardant (FR) additives. Consequently, extensive research efforts are dedicated to the development of synergistic systems, aiming to enhance flame retardancy while minimizing the total loading of FR additives

The mechanical properties of neat PP and the various composites were evaluated by tensile testing. The stress–strain curves are presented in Fig. 12, and the corresponding data are summarized in Table 6. The incorporation of 30 wt.% native cellulose into PP led to a significant loss in ductility, with elongation at break dropping from 55 % for neat PP to just 2.8 %. A similar trend was observed when phosphorylated celluloses MCC-P1 and MCC-P2 were incorporated, as the elongation at break remained low, around 4.7 % in both cases. The yield stress, an essential parameter reflecting the mechanical strength of polymers, also decreased markedly, from 17.1 MPa for neat PP to 10 MPa with native

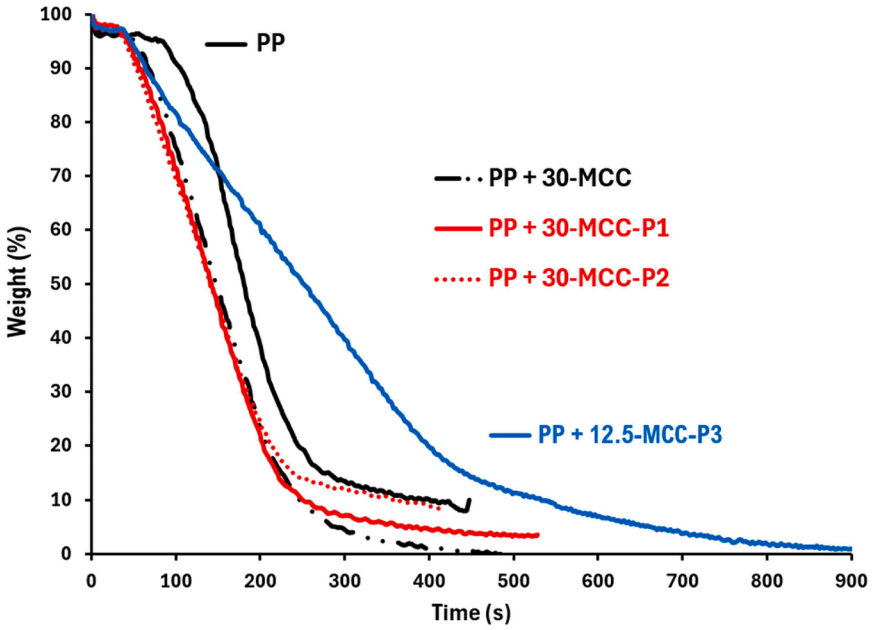

Fig. 10. Mass loss rate curves recorded during Mass Loss Calorimeter test.

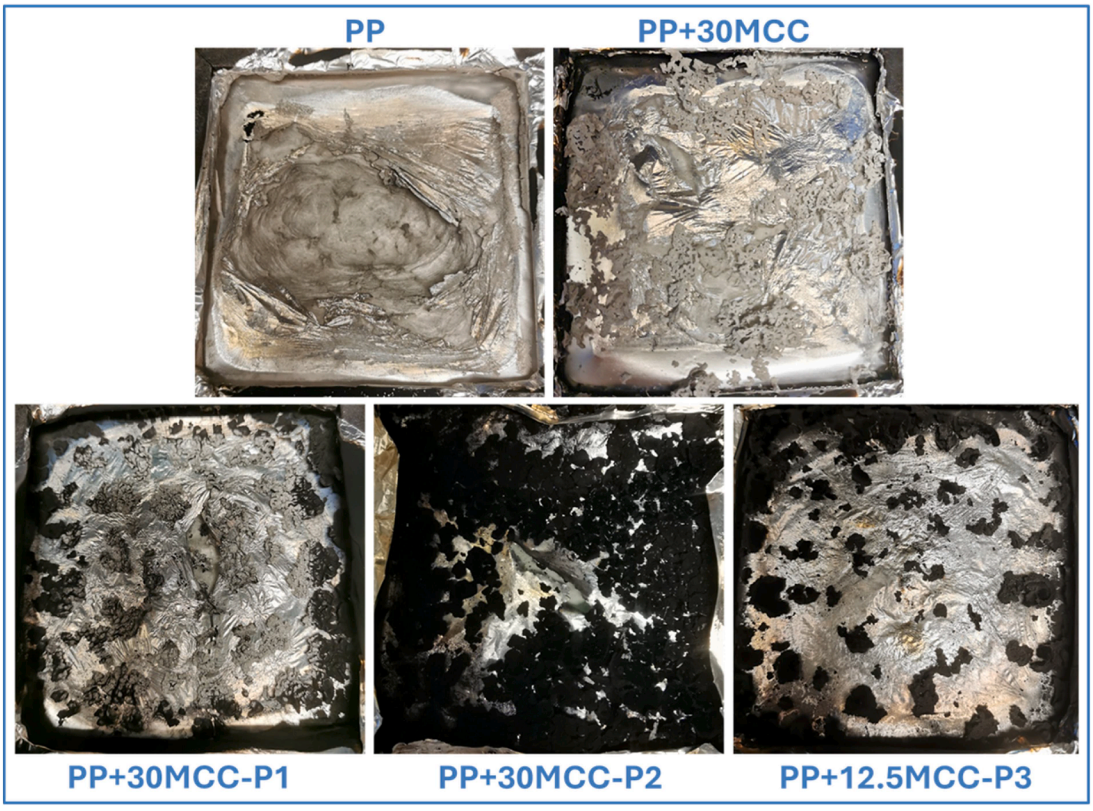

Fig. 11. Pictures of the tested samples at the end of the combustion during Mass Loss Cone calorimeter test.

cellulose, and to 11 MPa and 14.2 MPa for composites containing 30 wt.% of MCC-P1 and MCC-P2, respectively. These changes in mechanical properties clearly indicate a embrittlement of the PP matrix, caused by the presence of cellulose particles which act as stress concentrators and weaken the composite structure. In contrast, incorporating phosphorylated cellulose (MCC-P3) contributes to maintaining the ductility of the composite.

Only a slight decrease in maximum stress was observed, down to 15.2 MPa, which remains relatively minor. To assess whether the limited changes in mechanical properties were solely due to the lower incorporation rate of MCC-P3 (12.5 wt.%) compared to the 30 wt.% used for the other celluloses, a control composite containing 12.5 wt.% of unmodified cellulose was prepared and its mechanical properties evaluated. The results clearly show that the good mechanical performance of the 12.5 wt.% MCC-P3 composite cannot be attributed solely to its lower filler content. While the composite with 12.5 wt.% native cellulose

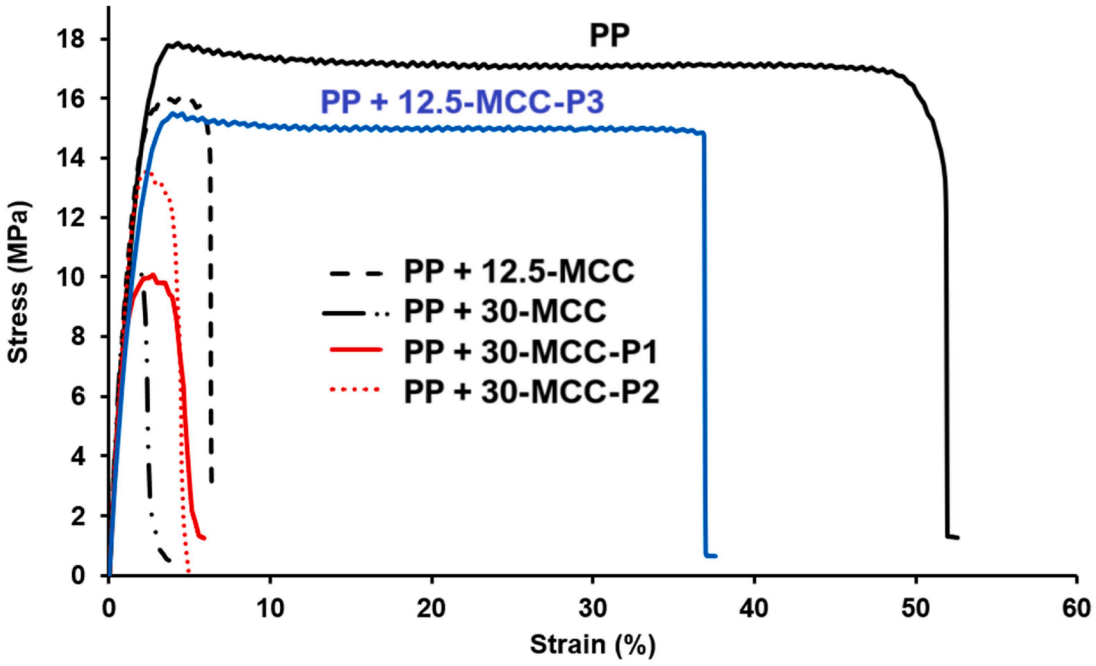

Fig. 12. Stress/strain curves of neat PP and PLA/Cellulose composites from tensile test.

Table 6
Young's modulus (E), tensile strength (σ_{max}), elongation at break (ε_{break}) from tensile test of PP and PP/cellulose composites.

Référence	E (MPa)	σ_{max} (MPa)	ε_{break} (%)
PP	1115 ± 50	17.5 ± 1	55 ± 17
PP + 30 MCC	1255 ± 80	10 ± 1	2.8 ± 0.3
PP + 12.5 MCC	1217 ± 64	16 ± 1	12 ± 2.3
PP + 30 MCC-P1	1000 ± 180	11 ± 2	4.7 ± 0.7
PP + 30 MCC-P2	1250 ± 105	14.2 ± 0.7	4.6 ± 1.2
PP + 12.5 MCC-P3	920 ± 10	15.2 ± 0.2	35.5 ± 3.2

exhibited better elongation at break than the composites loaded at 30 wt.%, it remained significantly lower than that of the PP–12.5 wt.% MCC-P3 system. These findings suggest that the enhanced mechanical behavior of the MCC-P3-based composite is not only a result of reduced filler loading, but also likely stems from intrinsic features of MCC-P3. Indeed, MCC-P3 exhibits a lower bulk density, a porous morphology, a graphitic-like structure, and a reduced hydroxyl group content, which renders the particles more hydrophobic and thus more compatible with polypropylene. These features may facilitate better mechanical interlocking between the phosphorylated cellulose particles and the polypropylene matrix. The inclusion of various grades of cellulose, irrespective of their incorporation rates, does not result in substantial variations in the Young's modulus, which fluctuates around the modulus value of PP, approximately 1100 MPa.

4. Conclusion

Through a mechanochemical approach, we achieved a remarkable effect that cannot be obtained using conventional solution-based reactions. Specifically, in the presence of a large excess of P_2O_5, the contact between cellulose-P_2O_5 mixture treated for 1 h by ball milling and a small amount of water triggered a vigorous reaction. This reaction led to the graphitization of cellulose, the grafting of a high phosphorus content (17.5 wt.%), and to the easy recovery of the modified cellulose, which precipitated readily in water. The cellulose produced under these conditions exhibited superior flame retardant performance compared to the other two phosphorylated celluloses prepared with lower amounts of P_2O_5. Notably, it also allowed the preservation of the mechanical properties of polypropylene in tensile tests. This study highlights the potential of mechanochemistry both as an effective tool for the chemical modification of bio-additives and as a promising approach for developing novel high-performance bio-based flame retardants.

Funding

This research was co-funded by the European Regional Development Fund (ERDF), the Wallonne region, and the Flemish region (Agentschap innoveren & ondernemen (VLAIO)), in the framework of the INTERREG FWVL V programme (VALCELMAT project 2024–2028 (https://valcelmat.eu/)).

CRediT authorship contribution statement

Sophie Dropsit: Project administration, Methodology, Investigation, Formal analysis, Data curation. **Jevgenij Lazko:** Writing – review & editing, Methodology, Funding acquisition. **Nicolas Landercy:** Investigation, Formal analysis, Data curation. **Philippe Dubois:** Writing – review & editing, Visualization, Supervision, Resources, Project administration. **Fouad Laoutid:** Writing – review & editing, Writing – original draft, Validation, Supervision, Methodology, Investigation, Funding acquisition, Conceptualization.

Declaration of competing interest

The authors declare the following financial interests/personal relationships which may be considered as potential competing interests: Laoutid fouad reports financial support was provided by the European Regional Development Fund (ERDF), the Wallonne region, and the Flemish region (Agentschap innoveren & ondernemen (VLAIO)), in the framework of the INTERREG FWVL V programme. If there are other authors, they declare that they have no known competing financial interests or personal relationships that could have appeared to influence the work reported in this paper.

Data availability

Data will be made available on request.

References

[1] L. Costes, F. Laoutid, S. Brohez, P. Dubois, Bio-based flame retardants: when nature meets fire protection, Mater. Sci. Eng. R Rep. 117 (2017) 1–25, https://doi.org/10.1016/j.mser.2017.04.001.

[2] V. Marturano, A. Marotta, S.A. Salazar, V. Ambrogi, P. Cerruti, Recent advances in bio-based functional additives for polymers, Prog. Mater. Sci. 139 (2023) 101186, https://doi.org/10.1016/j.pmatsci.2023.101186.

[3] M. Wang, G.Z. Yin, Y. Yang, W. Fu, J.L. Díaz Palencia, J. Zhao, N. Wang, Y. Jiang, D.Y. Wang, Bio-based flame retardants to polymers: a review, Adv. Ind. Eng. Polym. Res. 6 (2) (2023) 132–155, https://doi.org/10.1016/j.aiepr.2022.07.003.

[4] H. Meng, M. Wen, J. Shi, Y. Liang, H. Jian, Biomass flame retardants with application of cellulose, lignin, and hemicellulose from Wood Resources and their flame retardant technologies in related materials: a review, Sustain. Chem. Pharm. 42 (2024) 101816, https://doi.org/10.1016/j.scp.2024.101816.

[5] A. De Chirico, M. Armanini, P. Chini, G. Cioccolo, F. Provasoli, G. Audisio, Flame retardants for polypropylene based on lignin, Polym. Degrad. Stab. 79 (1) (2003) 139–145, https://doi.org/10.1016/S0141-3910(02)00266-5.

[6] F. Laoutid, V. Duriez, L. Brison, S. Aouadi, H. Vahabi, P. Dubois, Synergistic flame-retardant effect between lignin and magnesium hydroxide in poly(ethylene-Co-vinyl acetate, Flame Retard. Therm. Stab. Mater. 2 (1) (2019) 9–18, https://doi.org/10.1515/flret-2019-0002.

[7] W. Lu, Q. Li, Y. Zhang, H. Yu, S. Hirose, H. Hatakeyama, Y. Matsumoto, Z. Jin, Lignosulfonate/APP IFR and its flame retardancy in Lignosulfonate-based rigid polyurethane foams, J. Wood Sci. 64 (3) (2018) 287–293, https://doi.org/10.1007/s10086-018-1701-4.

[8] D. Liang, X. Zhu, P. Dai, X. Lu, H. Guo, H. Que, D. Wang, T. He, C. Xu, H.M. Robin, Z. Luo, X. Gu, Preparation of a novel lignin-based flame retardant for Epoxy resin, Mater. Chem. Phys. 259 (2021) 124101, https://doi.org/10.1016/j.matchemphys.2020.124101.

[9] N. Mandlekar, A. Cayla, F. Rault, S. Giraud, J. Guan, F. Salaün, Influence of char-forming lignin in combination with aluminium phosphinate on thermal stability and combustion properties of polyamide 11 blends, Fire Mater. 48 (3) (2024) 367–379, https://doi.org/10.1002/fam.3189.

[10] L. Costes, F. Laoutid, M. Aguedo, A. Richel, S. Brohez, C. Delvosalle, P. Dubois, Phosphorus and nitrogen derivatization as efficient route for improvement of lignin flame retardant action in PLA, Eur. Polym. J. 84 (2016) 652–667, https://doi.org/10.1016/j.eurpolymj.2016.10.003.

[11] M. Puyadena, P. Widsten, T. Wirtanen, M. Kellock, G. Ortega, A. Mugica, E. Matxinandiarena, I. Etxeberria, L. Martin, A. Agirre, A. Barrio, A. González, L. Irusta, Phosphorus-containing lignin intermediates as reactive bio-based flame-retardants for polyurethane and acrylic coatings for wood, Ind. Crops Prod. 220 (2024) 119261, https://doi.org/10.1016/j.indcrop.2024.119261.

[12] D. Aoki, Y. Nishio, Phosphorylated cellulose propionate derivatives as thermoplastic flame resistant/retardant materials: influence of regioselective phosphorylation on their thermal degradation behaviour, Cellulose 17 (5) (2010) 963–976, https://doi.org/10.1007/s10570-010-9440-8.

[13] L. Costes, F. Laoutid, F. Khelifa, G. Rose, S. Brohez, C. Delvosalle, P. Dubois, Cellulose/phosphorus combinations for sustainable fire retarded polylactide, Eur. Polym. J. 74 (2016) 218–228, https://doi.org/10.1016/j.eurpolymj.2015.11.030.

[14] T. Zhang, M. Wu, S. Kuga, C.M. Ewulonu, Y. Huang, Cellulose nanofibril-based flame retardant and its application to paper, ACS Sustain. Chem. Eng. 8 (27) (2020) 10222–10229, https://doi.org/10.1021/acssuschemeng.0c02892.

[15] F. Laoutid, V. Karaseva, L. Costes, S. Brohez, R. Mincheva, P. Dubois, Novel bio-based flame retardant systems derived from tannic acid, J. Renew. Mater. 6 (6) (2018) 559–572, https://doi.org/10.32604/JRM.2018.00004.

[16] J.F. Marques, A.F. Baldissera, M.R. Silveira, A.C. Dornelles, C.A. Ferreira, P. erformance of phosphorylated tannin-based intumescent coatings in passive fire protection, J. Coat. Technol. Res. 18 (3) (2021) 899–910, https://doi.org/10.1007/s11998-020-00440-2.

[17] H.B. Yuan, R.C. Tang, C.B. Yu, Flame retardant functionalization of microcrystalline cellulose by phosphorylation reaction with phytic acid, Int. J. Mol. Sci. 22 (17) (2021) 9631, https://doi.org/10.3390/ijms22179631.

[18] X. Liu, Y. Li, L. Zeng, X. Li, N. Chen, S. Bai, H. He, Q. Wang, C. Zhang, A review on mechanochemistry: approaching advanced energy materials with greener force, Adv. Mater 34 (46) (2022) 2108327, https://doi.org/10.1002/adma.202108327.

[19] L. Dong, L. Li, H. Chen, Y. Cao, H.Mechanochemistry Lei, Fundamental principles and applications, Adv. Sci. (2024) 2403949, https://doi.org/10.1002/advs.202403949.

[20] A. Krusenbaum, S. Grätz, G.T. Tigineh, L. Borchardt, J.G. Kim, T.he Mechanochemical synthesis of polymers, Chem. Soc. Rev. 51 (7) (2022) 2873–2905, https://doi.org/10.1039/D1CS01093J.

[21] M. Aaddouz, F. Laoutid, J. Mariage, B. Yada, A. Toncheva, J. Lazko, K. Azzaoui, R. Sabbahi, E. Mejdoubi, M.R. Saeb, P. Dubois, Mechanochemistry for the synthesis of a sustainable phosphorus/potassium tannic acid flame-retardant additive and its application in polypropylene, ACS Sustain. Chem. Eng. 13 (4) (2025) 1450–1459, https://doi.org/10.1021/acssuschemeng.4c04952.

[22] M. Aaddouz, F. Laoutid, J. Mariage, J. Lazko, B. Yada, E.M. Mejdoubi, A. Toncheva, P. Dubois, Facile preparation route of cellulose-based flame retardant by ball-milling mechanochemistry, Molecules 29 (24) (2024) 6065, https://doi.org/10.3390/molecules29246065.

[23] L. Costes, F. Laoutid, F. Khelifa, G. Rose, S. Brohez, C. Delvosalle, P. Dubois, Cellulose/phosphorus combinations for sustainable fire retarded polylactide, Eur. Polym. J. 74 (2016) 218–228, https://doi.org/10.1016/j.eurpolymj.2015.11.030.

[24] M. Aaddouz, F. Laoutid, J. Mariage, J. Lazko, B. Yada, E.M. Mejdoubi, A. Toncheva, P. Dubois, Facile preparation route of cellulose-based flame retardant by ball-milling mechanochemistry, Molecules 29 (24) (2024) 6065, https://doi.org/10.3390/molecules29246065.

[25] Comprehensive Cellulose Chemistry, Volume 2: Functionalization of Cellulose | Wiley. Wiley.com. https://www.wiley.com/en-be/Comprehensive+Cellulose+Chemistry%2C+Volume+2%3A+Functionalization+of+Cellulose-p-9783527601936 (accessed 2025-04-16).

[26] C. Pozo, J. Díaz-Visurraga, D. Contreras, J. Freer, J. Rodríguez, Characterization of temporal biodegradation of Radiata Pine by gloeophyllum trabeum through principal component analysis-based two-dimensional correlation ftir spectroscopy, J. Chil. Chem. Soc. 61 (2) (2016) 2878–2883, https://doi.org/10.4067/S0717-97072016000200006.

[27] K. Ahn, A. Schedl, T. Zweckmair, T. Rosenau, A. Potthast, Fire-induced structural changes and long-term stability of burned historical rag papers, Sci. Rep. 8 (1) (2018) 12036, https://doi.org/10.1038/s41598-018-30424-7.

[28] S. Soares, N.M.P.S. Ricardo, S. Jones, F. Heatley, High temperature thermal degradation of cellulose in air studied using FTIR and 1H and 13C solid-state NMR, Eur. Polym. J. 37 (4) (2001) 737–745, https://doi.org/10.1016/S0014-3057(00)00181-6.

[29] J. Feng, Z. Ma, Z. Xu, H. Xie, Y. Lu, C. Maluk, P. Song, S. Bourbigot, H. Wang, A Si-containing polyphosphoramide via green chemistry for fire-retardant polylactide with well-preserved mechanical and transparent properties, Chem. Eng. J. 431 (2022) 134259, https://doi.org/10.1016/j.cej.2021.134259.

[30] S. Stankovich, D.A. Dikin, R.D. Piner, K.A. Kohlhaas, A. Kleinhammes, Y. Jia, Y. Wu, S.T. Nguyen, R.S. Ruoff, S.ynthesis of graphene-based nanosheets via chemical reduction of exfoliated graphite oxide, Carbon. N Y 45 (7) (2007) 1558–1565, https://doi.org/10.1016/j.carbon.2007.02.034.

[31] A.M. Rao, E. Richter, S. Bandow, B. Chase, P.C. Eklund, K.A. Williams, S. Fang, K. R. Subbaswamy, M. Menon, A. Thess, R.E. Smalley, G. Dresselhaus, M. S. Dresselhaus, D.iameter-selective raman scattering from vibrational modes in carbon nanotubes, Science 275 (5297) (1997) 187–191, https://doi.org/10.1126/science.275.5297.187.

[32] S. Stankovich, D.A. Dikin, R.D. Piner, K.A. Kohlhaas, A. Kleinhammes, Y. Jia, Y. Wu, S.T. Nguyen, R.S. Ruoff, S.ynthesis of graphene-based nanosheets via chemical reduction of exfoliated graphite oxide, Carbon. N Y 45 (7) (2007) 1558–1565, https://doi.org/10.1016/j.carbon.2007.02.034.

[33] H.B. Yuan, R.C. Tang, C.B. Yu, Flame retardant functionalization of microcrystalline cellulose by phosphorylation reaction with phytic acid, Int. J. Mol. Sci. 22 (17) (2021) 9631, https://doi.org/10.3390/ijms22179631.

[34] H.A. Said, I. Ait Bourhim, A. Ouarga, I. Iraola-Arregui, M. Lahcini, A. Barroug, H. Noukrati, H. Ben Youcef, Sustainable phosphorylated microcrystalline cellulose toward enhanced removal performance of methylene blue, Int. J. Biol. Macromol. 225 (2023) 1107–1118, https://doi.org/10.1016/j.ijbiomac.2022.11.172.

[35] H. Ait Said, F.E. Bouharras, H. Derbani, S. Abouricha, J. El Karroumi, M. Lahcini, H. Noukrati, H. Ben Youcef, Highly phosphorylated cellulose toward efficient removal of cationic dyes from aqueous solutions, Int. J. Biol. Macromol. 280 (2024) 136116, https://doi.org/10.1016/j.ijbiomac.2024.136116.

[36] E.H. Ablouh, F. Brouillette, M. Taourirte, H. Sehaqui, M. El Achaby, A. Belfkira, A highly efficient chemical approach to producing green phosphorylated cellulosic macromolecules, RSC Adv. 11 (39) (2021) 24206–24216, https://doi.org/10.1039/D1RA02713A.

[37] G. Dobele, G. Rossinskaja, G. Telysheva, D. Meier, O. Faix, Cellulose dehydration and depolymerization reactions during pyrolysis in the presence of phosphoric acid, J. Anal. Appl. Pyroly. 49 (1) (1999) 307–317, https://doi.org/10.1016/S0165-2370(98)00126-0.

[38] D.Y. Kim, Y. Nishiyama, M. Wada, S. Kuga, High-yield carbonization of cellulose by sulfuric acid impregnation, Cellulose 8 (1) (2001) 29–33, https://doi.org/10.1023/A:1016621103245.

[39] W. Chaiwat, I. Hasegawa, T. Tani, K. Sunagawa, K. Mae, Analysis of cross-linking behavior during pyrolysis of cellulose for elucidating reaction pathway, Energ. Fuels 23 (12) (2009) 5765–5772, https://doi.org/10.1021/ef900674b.

[40] Y. Yamaguchi, C. Fushimi, K. Tasaka, T. Furusawa, A. Tsutsumi, Kinetic study on the pyrolysis of cellulose using the novel continuous cross-flow moving bed type differential reactor, Energ. Fuels 20 (6) (2006) 2681–2685, https://doi.org/10.1021/ef050334f.

[41] B.K. Kandola, A.R. Horrocks, D. Price, G.V. Coleman, F.lame-retardant treatments of cellulose and their influence on the mechanism of cellulose pyrolysis, J. Macromol. Sci. Part C 36 (4) (1996) 721–794, https://doi.org/10.1080/15321799608014859.